A GIS-based comparative evaluation of analytical hierarchy process and frequency ratio models for landslide susceptibility mapping

2 authors, including:

Qiqing Wang

China University of Mining and Technology

53 PUBLICATIONS   **1,050** CITATIONS

Some of the authors of this publication are also working on these related projects:

Influence of mining activities on eco-geological environment View project

A Special Issue for Journal Geofluids [SCI Index: JCR Q2, IF=1.534]: Behaviour and Composition of Fluids in Coal Mining View project
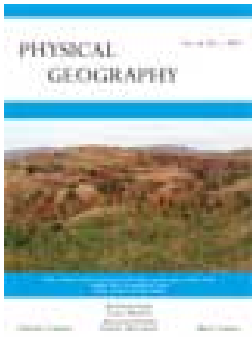
A GIS-based comparative evaluation of analytical hierarchy process and frequency ratio models for landslide susceptibility mapping

Qiqing Wang & Wenping Li

Taylor & Francis
Taylor & Francis Group

A GIS-based comparative evaluation of analytical hierarchy process and frequency ratio models for landslide susceptibility mapping

Qiqing Wang and Wenping Li

School of Resources and Geosciences, China University of Mining and Technology, Xuzhou, China

ABSTRACT

The purpose of this study is to assess the susceptibility of landslides in Wen County, China, using both analytical hierarchy process (AHP) and frequency ratio (FR) models. For this, a total of 529 landslides were identified and randomly split into two groups. The modeling group, which represented approximately 70% of the total landslides, was used as a training set to construct the susceptibility maps. The remaining 30% were used for validation purpose. Eight layers of landslide-related factors were prepared, including slope angle, altitude, distance to rivers, distance to roads, distance to faults, rainfall, lithology, and normalized difference vegetation index. Subsequently, landslide susceptibility maps were produced using the models. For verification, an area under curvature (AUC) and the seed cell area index (SCAI) assessments were applied. The AUC plot estimation results showed that the success rates of the AHP and FR models were 83.55 and 88.42% and the prediction rates were 83.43 and 86.62%, respectively. According to the validation results of the AUC and SCAI evaluations, the map obtained from the FR model is more accurate than that from the AHP model. These landslide susceptibility maps can be used for optimum management by decision makers and land-use planners.

1. Introduction

Landslides, often causing damages to residential regions, economic losses, and human fatalities, are much more common natural hazards in the world than any other natural disaster, including earthquakes, floods, volcanoes and windstorms (Nefeslioglu, Gokceoglu, & Sonmez, 2008; Solaimani, Mousavi, & Kavian, 2013). Likewise, there are frequent landslides in China, which often cause significant damage to people and property. It is reported that more than 5000 hazards associated with landslides occurred in the first half of 2015, resulting in more than 100 persons dead or missing and in economic losses of ¥7.3 billion. In the study area, landslides occur frequently due to special geomorphological, geological, and hydrogeological conditions. For instance, more than 20 hazards associated with landslides

---

occurred on 21 September 2010 in the Tielou township of Wen County, causing serious damage to many roads and large casualties. In this study area, a total of 529 landslides were identified and mapped (Figure 1). These landslides, mainly distributed along roads or rivers and concentrated in groups, were mainly shallow soil slips and debris flows. To date, not much work has been done on landslide susceptibility and risk analysis in Wen County. Therefore, it is necessary to assess the landslide susceptibility of the study area.

Nowadays, several techniques have been applied for landslide susceptibility mapping by many researchers (Nourani, Pradhan, Ghaffari, & Sharifi, 2014). These techniques can be divided into qualitative and quantitative methods (Yalcin, Reis, Aydinoglu, & Yomralioglu, 2011). Qualitative methods, including analytic hierarchy process and its combinations, such as multi-criteria evaluation (MCE) and multi-criteria decision analysis (MCDA), are based on heuristic approaches, which rely mainly on the experience of experts (Abella & Van Westen, 2007; Akgun, 2012; Erener, Mutlu, & Düzgün, 2015; Gorsevski & Jankowski, 2010; Kavzoglu, Sahin, & Colkesen, 2014; Park, Choi, Kim, & Kim, 2013; Pourghasemi, Moradi, Fatemi Aghda, Gokceoglu, & Pradhan, 2014; Pourghasemi, Pradhan, & Gokceoglu, 2012). Quantitative methods depend on obtaining the probability of sliding from quantitative techniques (Erener et al., 2015). These methods, including the frequency ratio model (Lee & Sambath, 2006; Pradhan & Lee, 2010; Yilmaz, 2009), logistic regression model (Ayalew & Yamagishi, 2005; Bui, Tuan, Klempe, Pradhan, & Revhaug, 2015), index of entropy model (Devkota et al., 2013; Wang, Li, Chen, & Bai, 2015), weights of evidence model (Dahal et al., 2008; Neuhäuser & Terhorst, 2007; Pradhan, Oh, & Buchroithner, 2010), decision tree
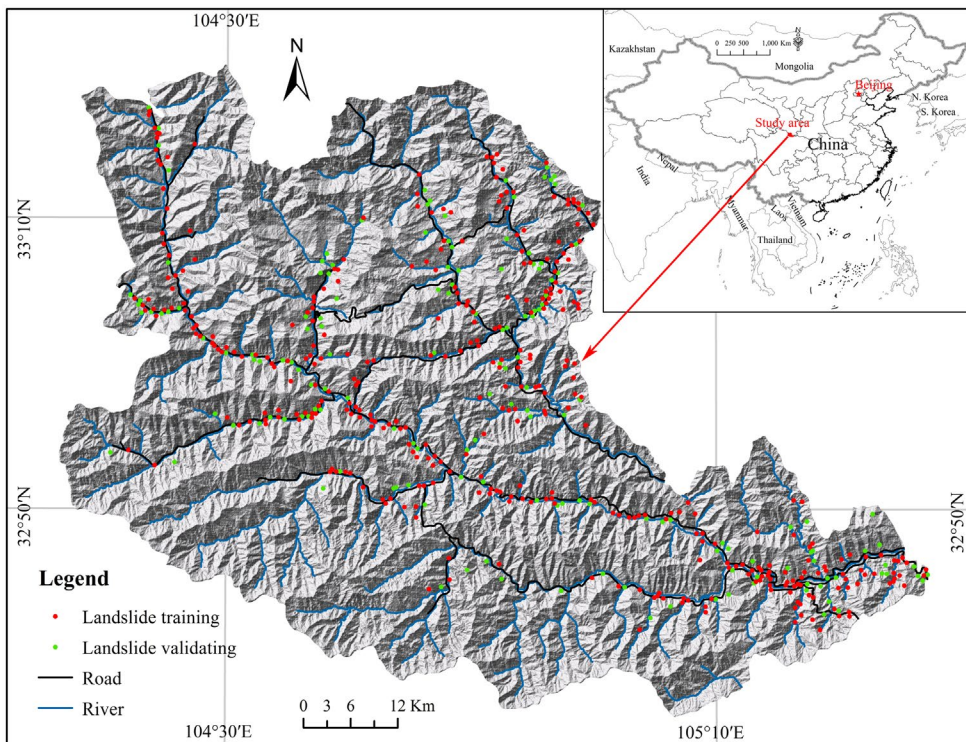
Figure 1. Location map of the study area.

model (Pradhan, 2013; Saito, Nakayama, & Matsuyama, 2009; Tsangaratos & Ilia, 2015), support vector machine (Bui et al., 2015; POURGHASEMI, JIRANDEH, PRADHAN, XU, & GOKCEOGLU, 2013; Yao, Tham, & Dai, 2008), bivariate statistics (Nandi & Shakoor, 2010; Yalcin, 2008; Yalcin et al., 2011), and multivariate analysis (Baeza & Corominas, 2001; Komac, 2006; Nandi & Shakoor, 2010) have been widely applied to landslide susceptibility mapping.

Determination of areas with high potential for landsliding can be used for optimum management by decision makers and land-use planners. Assessing the landslide susceptibility of the study area has been not done in the study area until now. This paper attempts to produce landslide susceptibility maps of Wen County, China, using the analytic hierarchy process (AHP) and frequency ratio (FR) methods, and based on a geographical information system (GIS). Landslide susceptibility maps produced by the two methods were compared and evaluated using validation data sets. The findings of the present study can be useful for the purpose of mitigating local hazards. Moreover, similar methods can be used elsewhere where the same topographical and geological features prevail.

2. Study area

Wen County, which is the study area, is located in the southeast of Gansu Province, China, (Figure 1) and covers an area of approximately 4994 km². The site lies between the latitudes 32°35′43″ and 33°20′36″N and the longitudes 104°16′16″ and 105°27′29″ E. The terrain of this study area is high in the west but low in the east. Mountainous terrain covers about 90% of the area. The basin floor is about 550 m a.s.l. and the highest peak is at 4187 m a.s.l. The climate is warm temperate humid monsoon, with mild a climate, four distinct seasons, hot and rainy summers, and cold and dry winters. The annual rainfall in this area is 400–800 mm, and the average summer and winter temperatures are estimated to be 24.8 and 3.6 °C, respectively. Within the boundary of the County, the Bailong and Baishui Rivers are among the larger river systems, running from west to east into the Jialing River, a tributary of the Yangtze River. By the end of 2012, the County had a total population of 240,900. Major settlements are distributed on both sides of the Bailong River, Baishui River, and their tributaries. In the study area, the landslides were mainly debris flows and shallow soil slips that occurred during or shortly after the days of high intensity rainfall.

3. Materials and methods

3.1. Landslide inventory

The key starting point in landslide susceptibility analysis is to prepare a landslide inventory map (Solaimani et al., 2013). Generally, landslide inventory maps can be produced either by collecting the information related to landslides or by analyzing satellite imagery and aerial photographs, coupled with field surveys (Pradhan & Kim, 2014). In this study, landslides (including potential landslides) in the study area were identified using 1:50,000-scale aerial-photo interpretations and field surveys. Additionally, historical records of landslides, obtained from the internet and published literature, were also used (Bi, 2014; Xie, 2013). According to our field observations, the historical landslides were still visible. A total of 529 landslides locations (including 82 potential landslides) were detected and mapped

(Figure 1), and medium-size landslides (volume < 0.1 million m³) and small landslides (volume > 0.1 million but < 10 million m³) accounted for about 80% of all landslides. Then, the inventory was randomly split into two datasets: 70% (370 landslide locations) was used for training the models and the remaining 30% (159 landslide locations) was used for validation purpose.

3.2. Spatial database construction

Determining the conditioning factors for landslides is crucial for developing a method for the assessment of landslide susceptibility (Ercanoglu & Gokceoglu, 2002; Shahabi, Hashim, & Ahmad, 2015). To produce a landslide susceptibility map, a spatial database that considers landslide-related factors, such as slope angle, altitude, distance to rivers, distance to roads, distance to faults, lithology, rainfall, and normalized difference vegetation index (NDVI), was designed and constructed.

The slope angle is regularly considered in landslide susceptibility studies since it is directly related to landslide incidence (Dai & Lee, 2001; He, Pan, Dai, Wang, & Liu, 2012). In this study, the slope map was extracted from the 25 m × 25 m digital elevation model (DEM) of the study area collected from the Advanced Space-borne Thermal Emission and reflection radiometer (ASTER). The slope angle of the study area was divided into six slope categories (Figure 2(a)). Altitude is also considered as another important factor in landslide susceptibility analysis. In general, altitude influences biological and natural factors, such as temperature, vegetation, and human activity. In turn, these conditions have the potential to affect slope stability and generate slope failure (Kavzoglu et al., 2014; Meng et al., 2015). In this study, the altitude of the study area derived from DEM was classified into six classes using 400-m intervals:<900, 900–1300, 1300–1700, 1700–2100, 2100–2500, and > 2500 m and is shown in Figure 2(b).

Three proximity parameters – distance to rivers, distance to roads, and distance to faults –were taken into account in the study. Distance to rivers is an important landslide conditioning factor. Streams can decrease slope stability and lead to landslide occurrence by eroding slopes or saturating the lower part of material until the water level increases (Dai & Lee, 2001; He et al., 2012; Solaimani et al., 2013). Similarly, the distance to roads is another important factor since the load in the toe of slope can be reduced by roadcuts (Yalcin et al., 2011). In this study, distances to rivers and roads were calculated by the Euclidean distance tool of ArcGIS 10.0 based on the drainage and road maps (1:50,000 scale), respectively. Six different buffer zones, with 200-m intervals, were created for the analysis (Figure 2(c) and (d)). Faults are responsible for triggering a large number of landslides because of the tectonic breaks that usually decrease the rock strength (Devkota et al., 2013; Qiao, Li, & Zhang, 2014). Generally speaking, landslides occur more frequently near faults (Meng et al., 2015). In this study, the distance-to-faults map was extracted from the geological map at 1:50,000 scale. Buffer intervals were set to 1000 m (Figure 2(e)).

Precipitation is considered to be a very important external triggering factor for landslide occurrence (van Westen, van Asch, & Soeters, 2006; Yang et al., 2015). In the present study, the average annual rainfall was used to characterize the precipitation factor. The annual rainfall of the study area is shown as Figure 2(f), and reclassified into four classes:<500, 500–600, 600–700, 700–800, and > 800 mm/year. Landslides are controlled by the rock properties of the land surface because different rock units have different landslide susceptibility values
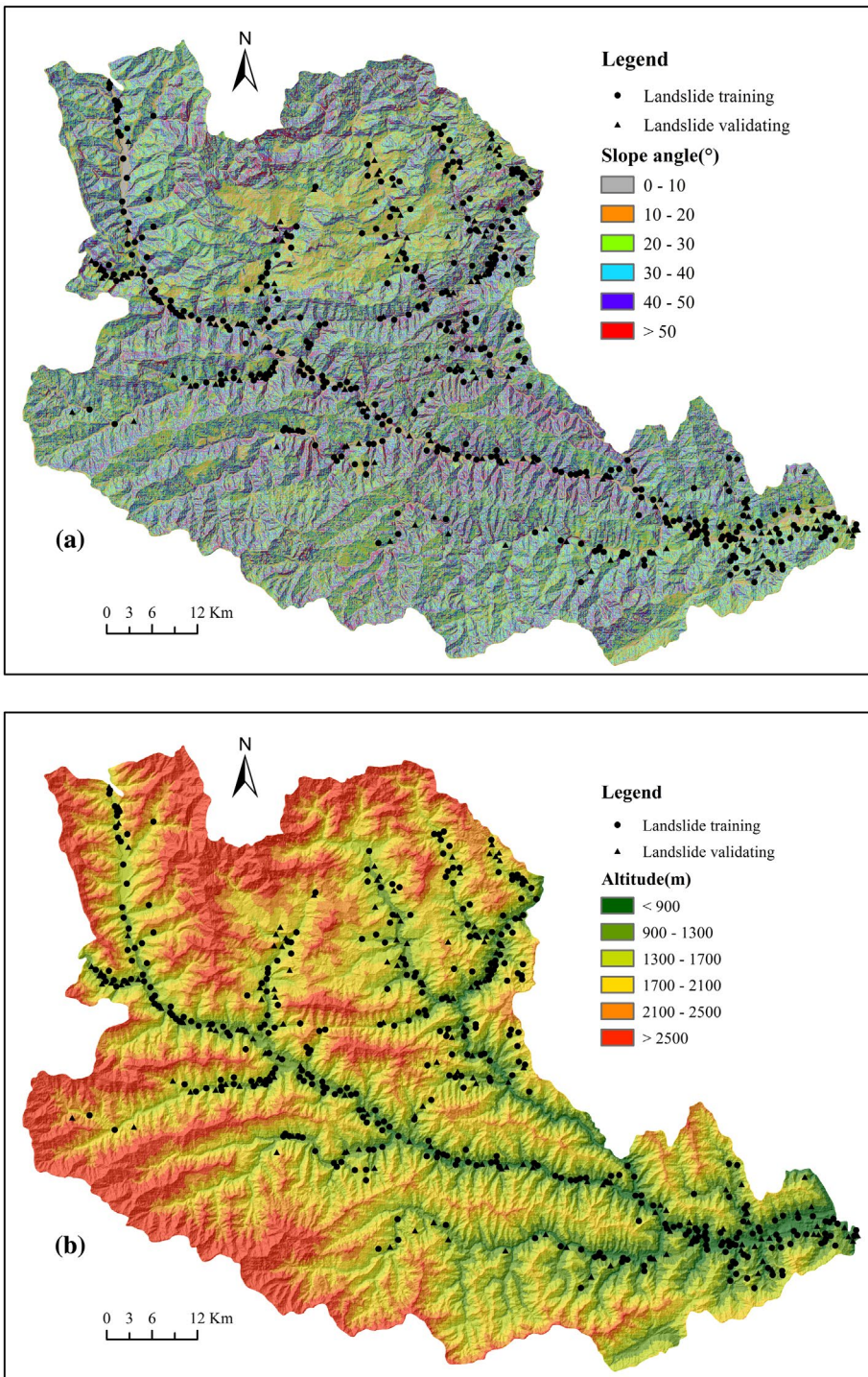
Figure 2. Maps of landslide susceptible conditioning factors: (a) slope angle; (b) altitude; (c) distance to rivers; (d) distance to roads; (e) distance to faults; (f) rainfall; (g) lithology; and (h) NDVI.
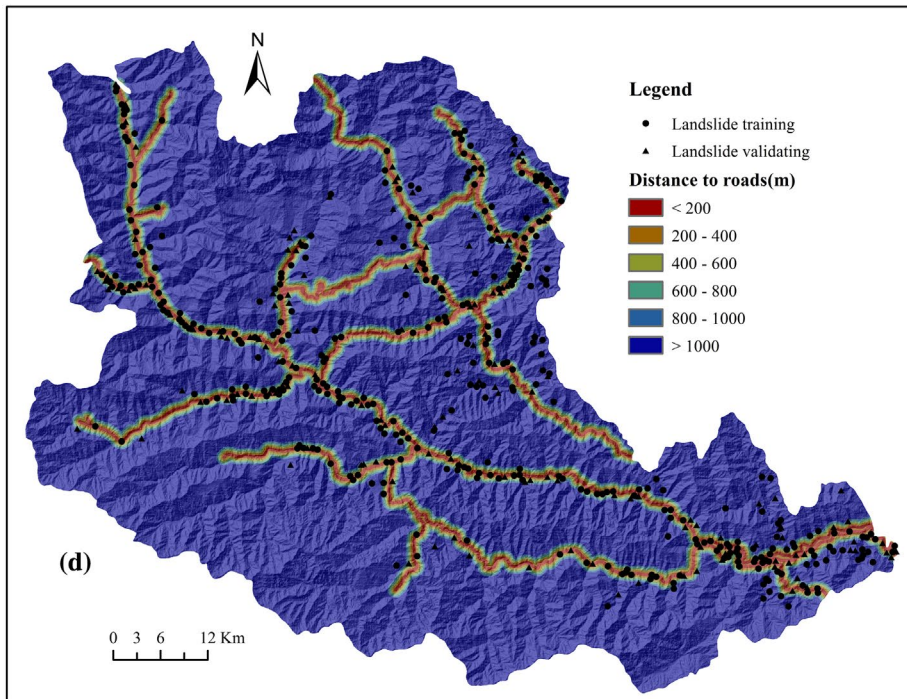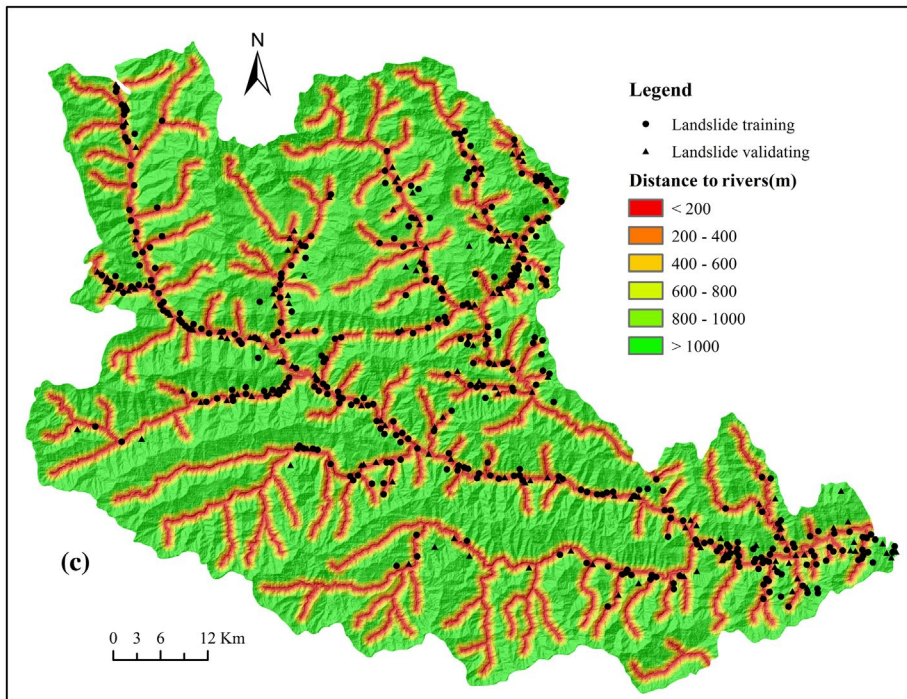
Figure 2. (*Continued*)
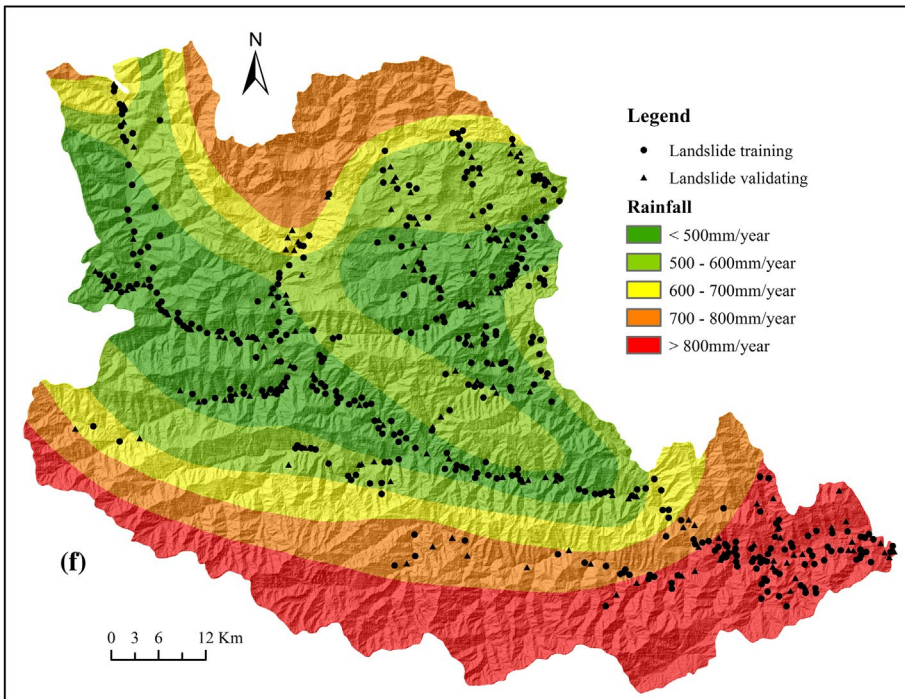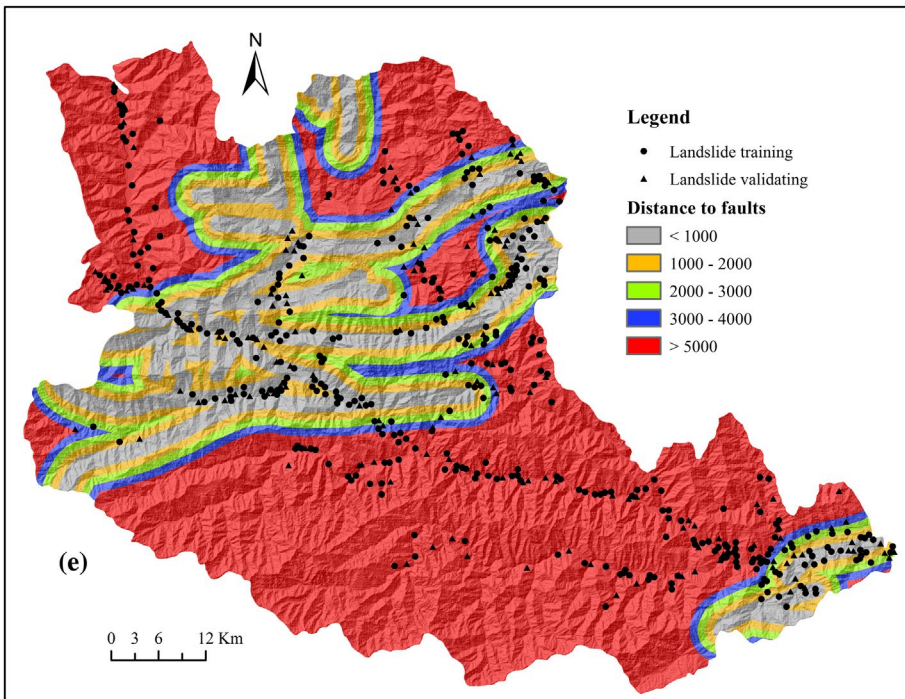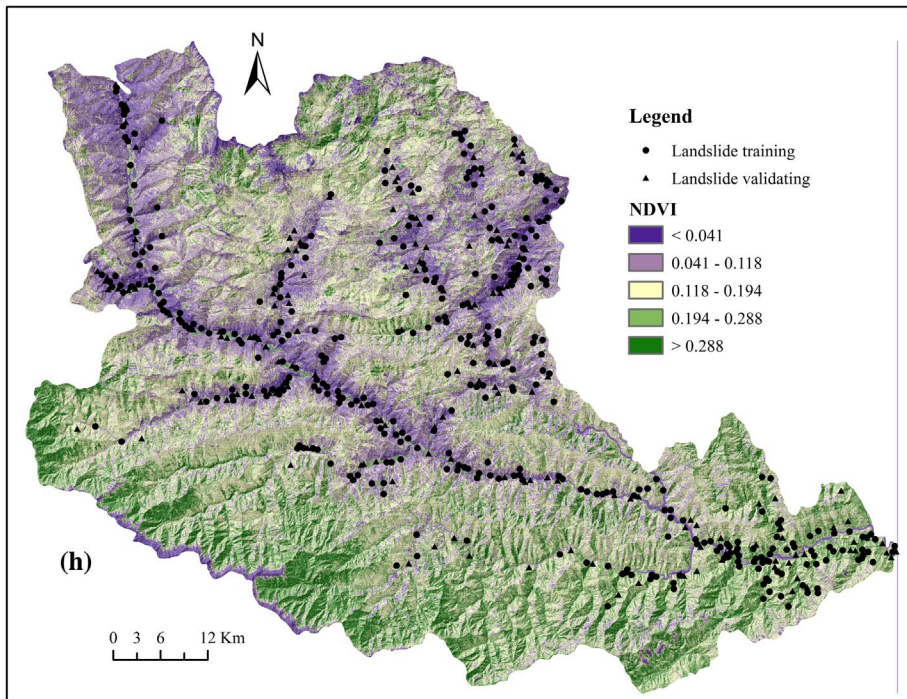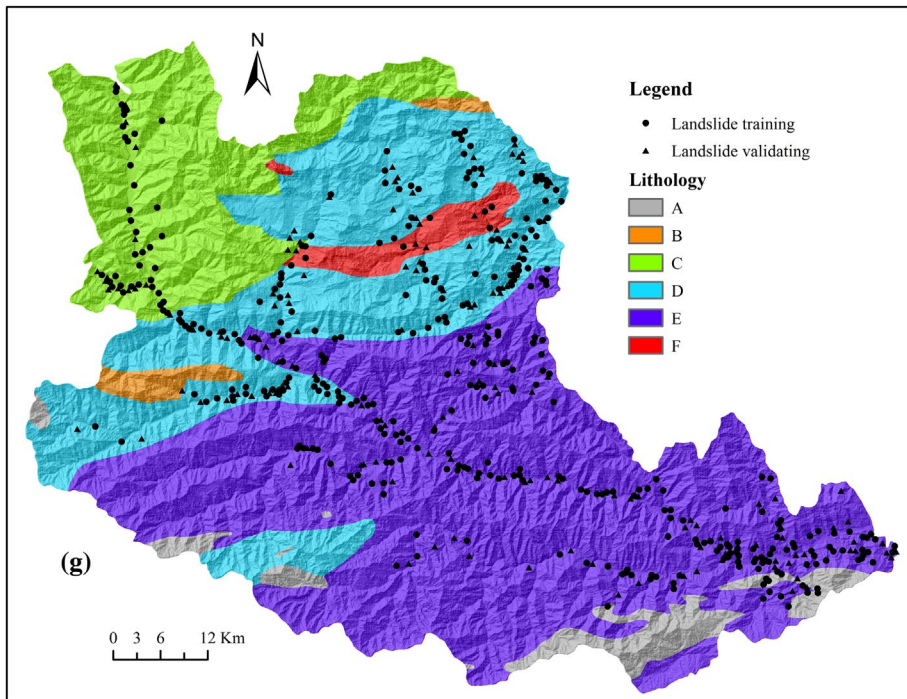
Figure 2. (*Continued*)

Figure 2. (*Continued*)

(Youssef, 2015). In this study, the lithology classification was prepared from a 1:50,000-scale geological map. The study area is covered with various types of lithological units (Figure 2(g)), and their names, lithologic characteristics, and ages of the geological units are given in Table 1.

The normalized difference vegetation index (NDVI) map was obtained from Landsat ETM+ satellite images from March 2009. The NDVI value was calculated using the formula:

$$NDVI = (IR - R)/(IR + R). \tag{1}$$

where IR is the infrared value and R is the red portion of the electromagnetic spectrum, respectively (Meng et al., 2015). The presence of dense green vegetation implies high NDVI values (Pradhan & Lee, 2010; Shahabi et al., 2015). In this study, the NDVI map was divided into four classes (Figure 2(h)).

3.3. Susceptibility mapping models

3.3.1. Analytical hierarchy process (AHP) model

The analytical hierarchy process (AHP) model, a simple decision-making tool to deal with complex, unstructured, and multi-attribute problems, was first developed by Saaty (1980). It has been widely applied in various fields of natural resources and environmental management (Karimi, Mehrdadi, Hashemian, Bidhendi, & Moghaddam, 2011; Lin & Shieh, 1995; Rahimdel & Ataei, 2014; Rahmati, Samani, Mahdavi, Pourghasemi, & Zeinivand, 2015; Zhang, Sun, & Qin, 2012). This model has been widely used in landslide susceptibility analysis, and procedures for applying it to landslide susceptibility have been detailed in the literature (Hasekioğulları & Ercanoglu, 2012; Kayastha, Dhital, & De Smedt, 2013; Ma, Wang, Yuan, Zhao, & Guo, 2013; Mansouri Daneshvar, 2014). The AHP requires the creation a of reciprocal pair-wise comparison matrix (Robinson, van Klinken, & Metternicht, 2010). To develop the pairwise comparison matrix, each landslide factor was rated against every other factor by assigning a relative dominant value ranging from 1 to 9 in accordance with the relative importance of the factors concerning landslide frequency. The value also varies between the reciprocals 1/2 and 1/9 for inverse comparison (Mondal & Maiti, 2013). In AHP, an index of consistency, known as the consistency ratio (CR), is used to indicate the probability that the matrix judgments were randomly generated (Saaty, 1980):

$$CR = CI/RI. \tag{2}$$

where RI is the average of the resulting consistency index depending on the order of the matrix given by Saaty (1980). The CI is the consistency index and can be expressed as:

$$CI = \left(\lambda_{\max} - n\right)/(n - 1). \tag{3}$$

Table 1. Description of geological units of the study area (Xie, 2013).

No.	Code	Lithology
A	γ, δ	The hard intrusive rocks
B	C	Layered hard and half hard limestone and dolomite
C	P_1, T	Layered, thin-layered, soft-hard sandy-slate, limestone and sandstone
D	D_2	Layered, thin-layered, soft-hard sandstone and shale, and carbonaceous-slate
E	P_{z1}	Layered, thin-layered, soft-hard fine-sandstone, phyllite and slate
F	J	Layered, soft conglomerate and shale

where λ_{max} is the largest eigenvalue of a preference matrix and n is the order of the matrix (Akgun, Dag, & Bulut, 2008). According to Saaty (1980), the *CR* should be < 0.1 to indicate the overall consistency of the pairwise comparison matrix, otherwise the comparison matrix should be revised (Mansouri Daneshvar, 2014).

In this study, expert analysis was used to score each major conditioning factor, using scoring criteria based on relative importance. Suggestions and opinions were collected and consulted from knowledgeable and experienced experts and colleagues from scientific research organizations. The eight conditioning factors represented by the digital maps have been ranked with respect to their impact on landsliding (Table 2). The last column of Table 2 is the weight values for each factor class. The weighting factor (W_j) values of each factor, given in Table 3, were determined. These weight values indicate the importance of a factor or a class. For instance, distance to roads is the most important conditioning factor followed by distance to roads, distance to rivers, NDVI, rainfall, distance to faults, while conditioning factors like lithology, slope angle, and altitude are less important. Finally, the landslide susceptibility index (LSI) is calculated according to the following equation (Ma et al., 2013; Pourghasemi et al., 2012):

$$
\begin{aligned}
\text{LSI} = &\left(\text{slope angle} \times 0.054\right) + (\text{altitude} \times 0.027) + (\text{distance to rivers} \times 0.187) \\
&+ (\text{distance to roads} \times 0.254) + (\text{distance to faults} \times 0.113) \\
&+ \left(\text{lithology} \times 0.077\right) + (\text{rainfall} \times 0.137) + (\text{NDVI} \times 0.149).
\end{aligned} \tag{4}
$$

3.3.2. Frequency ratio (FR) model

The frequency ratio model, a simple geospatial assessment tool, is based on the distribution of landslides and each landslide-related factor so that the correlation between the location of the landslide and the factors for the area can be represented (Lee & Pradhan, 2007; Saadatkhah, Kassim, & Lee, 2015; Youssef, Al-Kathery, & Pradhan, 2015). Firstly, the frequency ratios (a/b) for the class of each factor were calculated by dividing the landslide occurrence ratio (a) by the area ratio (b) (Akgun et al., 2008). A value of 1 is an average value. If the value is greater than 1, it means a high correlation, and a value lower than 1 indicates lower correlation (Nourani et al., 2014). Then the landslide susceptibility index was calculated by a summation of each factor ratio value as:

$$
\text{LSI} = FR_1 + FR_2 + FR_3 + \cdots + FR_n. \tag{5}
$$

where LSI is the landslide susceptibility index, *FR* is the frequency ratio of a factor, and n is the total number of the landslide-related factors (Ozdemir & Altural, 2013).

4. Results and discussion

4.1. Landslide susceptibility mapping using analytical hierarchy process model

The LSI value of the study area ranged from 0.046 to 0.410. For zonation of the study area, the values acquired were reclassified into five relative susceptibility classes: very low, low, moderate, high, and very high using the natural break method (Figure 3). According to the landslide susceptibility map produced from the AHP model, 29.61% of the total area is found to have very low landslide susceptibility. Low, moderate, and high susceptible zones represent 35.28, 20.12, and 10.24% of the total area, respectively. The very high landslide susceptibility area is 4.75% of the total study area.

Table 2. Pair-wise comparison matrix, AHP weightings, and consistency ratio of factor classes.

Conditioning factors	Classes	(1)	(2)	(3)	(4)	(5)	(6)	Weightings
Slope angle(°)	(1) 0–10	1						0.064
	(2) 10–20	3	1					0.194
	(3) 20–30	5	2	1				0.391
	(4) 30–40	3	1	1/3	1			0.181
	(5) 40–50	2	1/2	1/4	1/2	1		0.107
	(6) >50	1	1/3	1/5	1/3	1/2	1	0.064
	Consistency ratio: 0.008							
Altitude(m)	(1) <900	1						0.207
	(2) 900–1300	2	1					0.341
	(3) 1300–1700	1	1/2	1				0.207
	(4) 1700–2100	1/2	1/3	1/2	1			0.122
	(5) 2100–2500	1/3	1/4	1/3	1/2	1		0.075
	(6) >2500	1/4	1/5	1/4	1/3	1/2	1	0.049
	Consistency ratio: 0.011							
Distance to rivers(m)	(1) 0–200	1						0.450
	(2) 200–400	1/2	1					0.236
	(3) 400–600	1/5	1/2	1				0.157
	(4) 600–800	1/7	1/3	1/3	1			0.086
	(5) 800–1000	1/8	1/5	1/5	1/3	1		0.045
	(6) >1000	1/9	1/7	1/6	1/5	1/3	1	0.026
	Consistency ratio: 0.056							
Distance to roads(m)	(1) 0–200	1						0.431
	(2) 200–400	1/2	1					0.241
	(3) 400–600	1/4	1/2	1				0.166
	(4) 600–800	1/6	1/3	1/3	1			0.090
	(5) 800–1000	1/8	1/5	1/5	1/3	1		0.046
	(6) >1000	1/9	1/7	1/6	1/5	1/3	1	0.026
	Consistency ratio: 0.048							
Distance to faults(m)	(1) 0–1000	1						0.489
	(2) 1000–2000	1/3	1					0.256
	(3) 2000–3000	1/4	1/3	1				0.141
	(4) 3000–4000	1/6	1/4	1/3	1			0.069
	(5) >4000	1/7	1/5	1/4	1/2	1		0.046
	Consistency ratio:0.045							
Lithology	(1) A	1						0.077
	(2) B	1/5	1					0.023
	(3) C	2	7	1				0.124
	(4) D	4	8	3	1			0.391
	(5) E	3	9	2	1/3	1		0.219
	(6) F	3	9	2	1/4	1/2	1	0.166
	Consistency ratio: 0.053							
Rainfall(mm/yr)	(1) <500	1						0.062
	(2) 500–600	2	1					0.097
	(3) 600–700	3	2	1				0.160
	(4) 700–800	4	3	2	1			0.263
	(5) >800	5	4	3	2	1		0.417
	Consistency ratio: 0.015							
NDVI	(1) <0.041	1						0.417
	(2) 0.041–0.118	1/2	1					0.263
	(3) 0.118–0.194	1/3	1/2	1				0.160
	(4) 0.194–0.288	1/4	1/3	1/2	1			0.097
	(5) >0.288	1/5	1/4	1/3	1/2	1		0.062
	Consistency ratio: 0.015							

4.2. Landslide susceptibility mapping using frequency ratio model

The calculated frequency ratios of each conditioning factor's classes, shown in Table 4, show the importance of the respective classes in the slope instability. It can be observed from Table 4 that the slope angle class 20–30° has the highest value of FR (1.467) and slope class > 50° has the lowest value of FR (0.158). This means that landslide occurrence increases by the increase in slope angle up to a certain extent, and then decreases. A similar trend
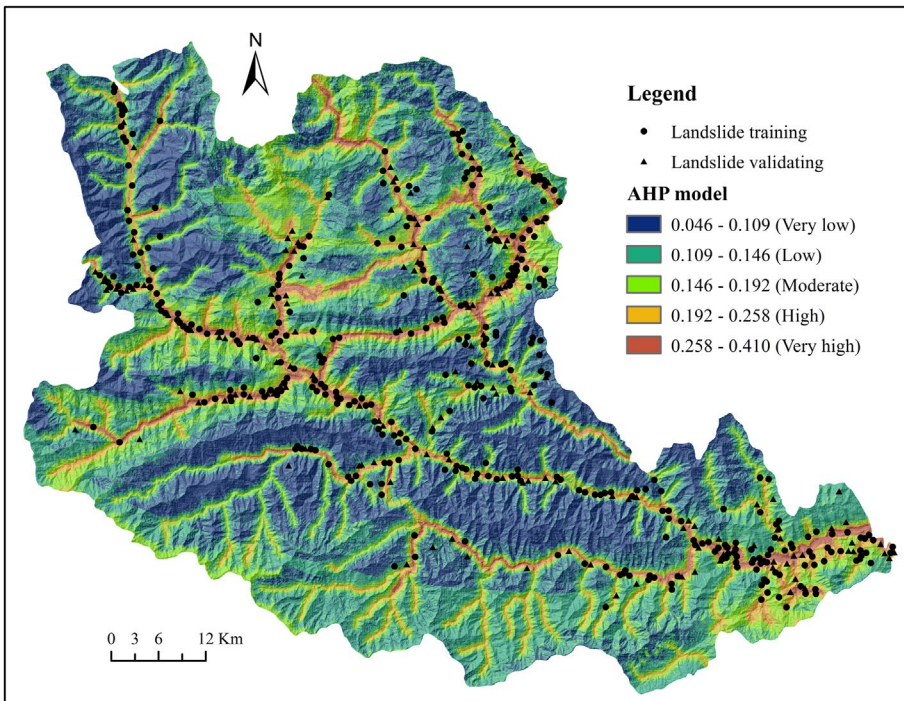
Figure 3. Landslide susceptibility map produced by the AHP model.

Table 3. The weight (W_j) of each landslide conditioning factors by AHP model.

Criteria	(1)	(2)	(3)	(4)	(5)	(6)	(7)	(8)	W_j
(1) Slope angle	1								0.054
(2) Altitude	1/3	1							0.027
(3) Distance to rivers	4	7	1						0.187
(4) Distance to roads	5	8	2	1					0.254
(5) Distance to faults	3	6	1/2	1/3	1				0.113
(6) Lithology	2	5	1/3	1/4	1/2	1			0.077
(7) Rainfall	4	7	1	1/2	1	2	1		0.137
(8) NDVI	3	6	1/2	1/2	2	3	2	1	0.149
Consistency ratio: 0.037									

was also found in the literature (Kanungo, Sarkar, & Sharma, 2011; Wang et al., 2015). For altitudes above 900 m, the frequency ratio was 7.232, which indicates a very high probability of landslide occurrence. In the case of the relationship between landslide occurrence and distance to rivers, as the distance to rivers increases, the landslide probability generally decreases. At a distance of < 200 m, the ratio was > 1, indicating a high probability of landslide occurrence, and at distances > 1000 m, the ratio was < 1, indicating a lower probability. Similarly, for distance to roads, the closer the road, the greater is the landslide probability. At a distance of < 200 m, the ratio was 6.808, indicating a high probability of a landslide. The ratio was < 1 at a distance > 1000 m, and this indicates a low probability. For distance to faults, the frequency ratio was highest (1.24) at distance of < 1000 m. In the case of rainfall, the landslide occurrence values were higher in the < 500 mm/year class. In case of lithology, groups D and E (see in details in Table 1) have a high frequency ratio (1.323,

Table 4. Frequency ratio (FR) values of the landslide-conditioning parameters.

Conditioning factors	Classes	Percentage of domain (%)	Percentage of landslide (%)	FR
Slope angle (°)	0–10	5.936	5.405	0.911
	10–20	16.537	22.162	1.340
	20–30	25.241	37.027	1.467
	30–40	26.891	19.189	0.714
	40–50	18.571	15.135	0.815
	>50	6.823	1.081	0.158
Altitude (m)	< 900	4.186	30.270	7.232
	900–1300	13.653	36.216	2.653
	1300 –1700	22.114	25.676	1.161
	1700–2100	25.096	7.838	0.312
	2100–2500	18.036	0.000	0.000
	> 2500	16.915	0.000	0.000
Distance to rivers (m)	< 200	10.863	38.649	3.558
	200–400	9.778	26.757	2.737
	400–600	9.430	11.081	1.175
	600–800	9.283	8.919	0.961
	800–1000	8.837	5.135	0.581
	> 1000	51.809	9.459	0.183
Distance to roads (m)	< 200	4.644	31.622	6.808
	200–400	4.085	17.568	4.301
	400–600	3.871	12.162	3.142
	600–800	3.824	9.730	2.544
	800–1000	3.715	4.865	1.309
	> 1000	79.859	24.054	0.301
Distance to faults (m)	< 1000	14.306	24.865	1.738
	1000–2000	11.470	15.405	1.343
	2000–3000	8.565	9.189	1.073
	3000–4000	6.928	4.054	0.585
	> 4000	58.730	46.486	0.792
Rainfall (mm/yr)	< 500	25.561	47.297	1.850
	500–600	23.749	21.351	0.899
	600–700	12.240	5.676	0.464
	700–800	18.091	5.135	0.284
	> 800	20.359	20.541	1.009
Lithology[a]	A	4.072	2.162	0.531
	B	1.354	0.000	0.000
	C	15.975	10.541	0.660
	D	25.935	34.324	1.323
	E	50.290	50.811	1.010
	F	2.374	2.162	0.911
NDVI	< 0.041	10.742	28.649	2.667
	0.041–0.118	26.562	32.703	1.231
	0.118–0.194	31.002	15.405	0.497
	0.194–0.288	21.717	12.432	0.572
	> 0.288	9.976	10.811	1.084

[a]Lithologies are described in Table 1.

1.010), which indicates that the probability of landslide occurrence in these lithological units is high. For group B of lithology, the ratio was 0.00, showing that these lithological units are not susceptible to landslide. In the case of NDVI, the frequency ratio was 2.667 for NDVI values < 0.041, which indicates a high landslide occurrence probability. For NDVI values between 0.118 and 0.194, the frequency ratio was 0.497, indicating a low landslide occurrence probability.

Landslide susceptibility index (LSI) values, ranging from 2.215 to 26.643, were classified by the natural break method and grouped into five susceptibility classes for visual interpretation: very low, low, moderate, high, and very high. In the landslide susceptibility map produced from the index of entropy model (Figure 4), the very low susceptibility zone covers
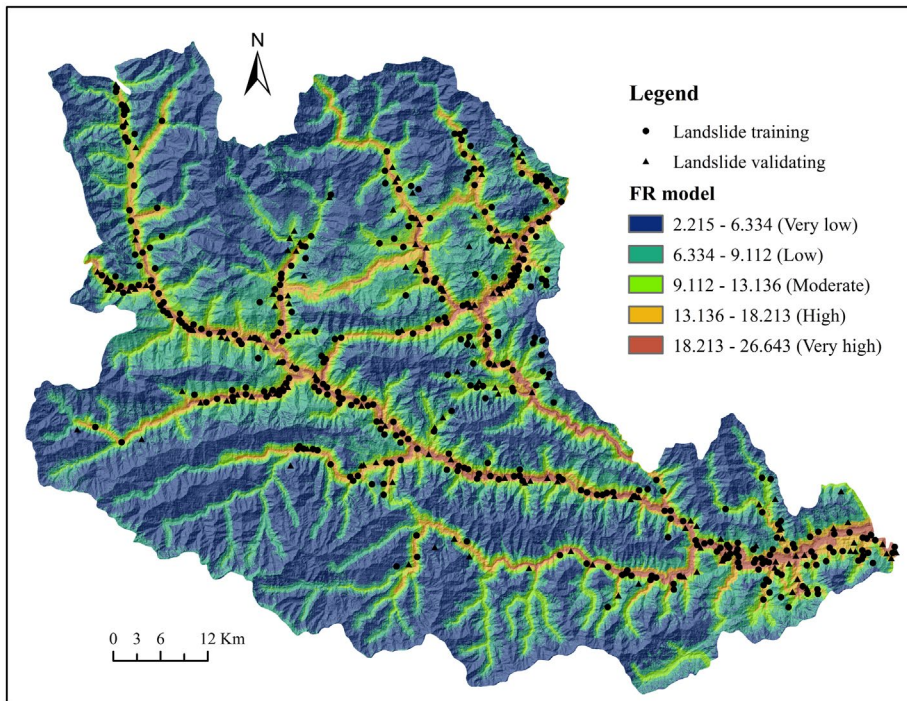
Figure 4. Landslide susceptibility map produced by the FR model.

44.36% of the total study area; whereas low, moderate, high, and very high susceptibility zones cover 30.56, 14.05, 7.32, and 3.71% of the total area, respectively.

4.3. Verification and comparison of the landslide susceptibility mapping

A proper validation is required to produce a certain landslide susceptibility map for any area (Youssef, Pourghasemi, El-Haddad, & Dhahry, 2015). In this study, validation and comparison of the landslides susceptibility maps produced by AHP and FR models were checked by using the area under curvature (AUC) and the seed cell area index (SCAI) methods (Chung & Fabbri, 1999; Kamp, Owen, Growley, & Khattak, 2010; van Westen, Rengers, & Soeters, 2003). The area-under-curvature (AUC) method works by creating success rate and prediction rate curves. Rate curves show the cumulative percentage of observed landslide occurrences (x-axis) versus cumulative percentage of decreasing landslide susceptibility index value (y-axis) (Kamp et al., 2010; Kayastha, Dhital, & De Smedt, 2012). For validation using the AUC method, the total landslides observed in the study area were divided into two groups: 70 and 30% of 529 landslide locations were used for training and validation of models, respectively. Success rate and prediction rate curves were created on the basis of training data and validating data, respectively, and their AUC were calculated (Figure 5). The success rate curve showed that the FR model has a higher area under the curve (AUC) value (88.42%) than the AHP model (83.55%). The prediction rate curve showed that prediction accuracy was 83.43 and 86.62% for AHP and FR models, respectively. From the evaluation results of the AUC method, it can be seen that the FR model exhibited a better result than
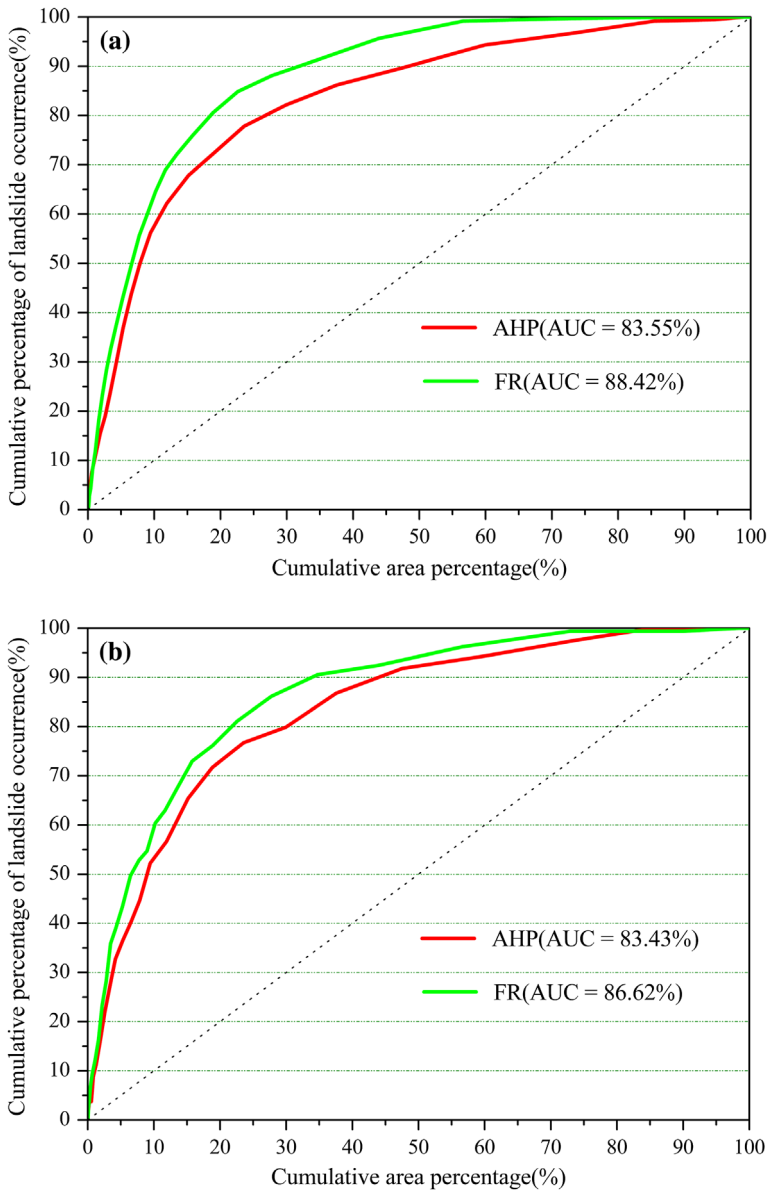
Figure 5. AUC representing quality model (a) success rate curve and (b) prediction rate curve.

AHP model for landslide susceptibility mapping in the study area. In order to compare the results of the two models, the seed cell area index (SCAI) method, proposed by Süzen and Doyuran (2004), also was applied. The SCAI value, as presented in Table 5, is simply the density of landslides among the classes and is calculated by dividing the susceptibility class area percent values by the landslide seed cell percent values (Chen et al., 2016; Conforti, Robustelli, Muto, & Critelli, 2012; Yilmaz, Topal, & Süzen, 2012). Generally, the produced maps are accurate when the high and very high susceptibility classes have very low SCAI values, whereas the SCAI values of the very low and low susceptibility classes are very high

Table 5. The densities of landslide occurrence among the landslide susceptibility classes for AHP and FR models.

Susceptibility classes	Area (%)		Seed (%)		SCAI	
	AHP	FR	AHP	FR	AHP	FR
Very low	29.61	44.36	3.97	2.08	7.46	21.33
Low	35.28	30.56	11.15	11.91	3.16	2.57
Moderate	20.12	14.05	17.96	20.23	1.12	0.69
High	10.24	7.32	32.51	31.38	0.31	0.23
Very High	4.75	3.71	34.40	34.40	0.14	0.11

(Akgun, 2012; Conforti et al., 2012; Pourghasemi et al., 2014). Therefore, it can also be seen from Table 5 that the map obtained from the FR model is more accurate than that from the AHP model for landslide susceptibility mapping.

The FR model is a quantitative method, based on the objective analysis of the relationship between landslide-related factors and many landslides. Therefore, it can objectively reflect the relationship between landslide distribution and landslide-related factors so that the assessment of landslide susceptibility is closer to the objective reality. The AHP model is a qualitative method. It relies on personal experience of reviewers who require a considerable understanding of the causes of landslides. Therefore, this method seriously relies on the experience of experts. The result of the evaluation, including evaluation rule selection and factor weight determination, also has some subjectivity. Generally, with more data of landslide locations in the study area, it is more suitable to use the FR method. In addition, there should be an emphasis on the models developed on some basic assumptions, including topography, geology, and streams. If data (factors causing the landslides, such as extreme rainfall, earthquake shaking) could be added to the models, then a more accurate analysis could be done. Furthermore, each factor classification method has more or less influence on the evaluation results. It needs to be further studied and optimized in a future study.

5. Conclusion

In the present study, two landslide susceptibility mapping models, the AHP and the FR models, were applied to Wen County, China, as the study area, using a GIS for estimating the susceptible areas of the study area. Their performances were analyzed through comparisons. The relationship between a landslide occurrence and the identified eight conditioning factors of slope angle, altitude, distance to rivers, distance to roads, distance to faults, rainfall, lithology, and normalized difference vegetation index (NDVI) was evaluated using the AHP and FR methods. In this process, a total of 529 landslides were mapped, out of which 370 (70%) were randomly selected to build landslide susceptibility models, while the remaining 159 (30%) were applied to validate the models. Landslide susceptibility maps produced by the AHP and FR models classified the study area into five zones, with susceptibility degrees of very low, low, moderate, high, and very high. To validate the prediction accuracy of the applied models, the obtained maps were compared with actual landslide locations, and the verification results were quantitatively analyzed using the AUC and SCAI methods. The AUC plot estimation results showed that the two models applied in this study showed reasonably good accuracy, with the FR model as the better one. According to the comparison of the susceptibility maps, by using the seed cell area index (SCAI) method, the FR model

also exhibited higher performance than the AHP model. The landslide susceptibility maps thus produced can be used to mitigate hazards associated with landslides and to land-cover planning.

Acknowledgements

Disclosure statement

No potential conflict of interest was reported by the authors.

References

Abella, E. C., & Van Westen, C. J. (2007). Generation of a landslide risk index map for Cuba using spatial multi-criteria evaluation. *Landslides, 4*, 311–325.

Akgun, A. (2012). A comparison of landslide susceptibility maps produced by logistic regression, multi-criteria decision, and likelihood ratio methods: A case study at İzmir, Turkey. *Landslides, 9*, 93–106.

Akgun, A., Dag, S., & Bulut, F. (2008). Landslide susceptibility mapping for a landslide-prone area (Findikli, NE of Turkey) by likelihood-frequency ratio and weighted linear combination models. *Environmental Geology, 54*, 1127–1143.

Ayalew, L., & Yamagishi, H. (2005). The application of GIS-based logistic regression for landslide susceptibility mapping in the Kakuda-Yahiko Mountains, Central Japan. *Geomorphology, 65*, 15–31.

Baeza, C., & Corominas, J. (2001). Assessment of shallow landslide susceptibility by means of multivariate statistical techniques. *Earth Surface Processes and Landforms, 26*, 1251–1263.

Bi, Y. H. (2014). *Study on evaluation and control of Nanshan geologic hazards of Wen County* (Master's thesis). Lanzhou University.

Bui, D. T., Tuan, T. A., Klempe, H., Pradhan, B., & Revhaug, I. (2015). Spatial prediction models for shallow landslide hazards: A comparative assessment of the efficacy of support vector machines, artificial neural networks, kernel logistic regression, and logistic model tree. *Landslides, 13*, 361–378.

Chen, W., Li, W., Chai, H., Hou, E., Li, X., & Ding, X. (2016). GIS-based landslide susceptibility mapping using analytical hierarchy process (AHP) and certainty factor (CF) models for the Baozhong region of Baoji City, China. *Environmental Earth Sciences, 75*, 1–14.

Chung, C. J. F., & Fabbri, A. G. (1999). Probabilistic prediction models for landslide hazard mapping. *Photogrammetric Engineering and Remote Sensing, 65*, 1389–1399.

Conforti, M., Robustelli, G., Muto, F., & Critelli, S. (2012). Application and validation of bivariate GIS-based landslide susceptibility assessment for the Vitravo river catchment (Calabria, south Italy). *Natural Hazards, 61*, 127–141.

Dahal, R. K., Hasegawa, S., Nonomura, A., Yamanaka, M., Masuda, T., & Nishino, K. (2008). GIS-based weights-of-evidence modelling of rainfall-induced landslides in small catchments for landslide susceptibility mapping. *Environmental Geology, 54*, 311–324.

Dai, F. C., & Lee, C. F. (2001). Terrain-based mapping of landslide susceptibility using a geographical information system: a case study. *Canadian Geotechnical Journal, 38*, 911–923.

Mansouri Daneshvar, M. R. M. (2014). Landslide susceptibility zonation using analytical hierarchy process and GIS for the Bojnurd region, northeast of Iran. *Landslides, 11*, 1079–1091.

Devkota, K. C., Regmi, A. D., Pourghasemi, H. R., Yoshida, K., Pradhan, B., Ryu, I. C., … Althuwaynee, O. F. (2013). Landslide susceptibility mapping using certainty factor, index of entropy and logistic

regression models in GIS and their comparison at Mugling-Narayanghat road section in Nepal Himalaya. *Natural Hazards, 65*, 135–165.

Ercanoglu, M., & Gokceoglu, C. (2002). Assessment of landslide susceptibility for a landslide-prone area (north of Yenice, NW Turkey) by fuzzy approach. *Environmental Geology, 41*, 720–730.

Erener, A., Mutlu, A., & Düzgün, H. S. (2015). A comparative study for landslide susceptibility mapping using GIS-based multi-criteria decision analysis (MCDA), logistic regression (LR) and association rule mining (ARM). *Engineering Geology, 203*, 45–55.

Gorsevski, P. V., & Jankowski, P. (2010). An optimized solution of multi-criteria evaluation analysis of landslide susceptibility using fuzzy sets and Kalman filter. *Computers & Geosciences, 36*, 1005–1020.

Hasekioğulları, G. D., & Ercanoglu, M. (2012). A new approach to use AHP in landslide susceptibility mapping: A case study at Yenice (Karabuk, NW Turkey). *Natural Hazards, 63*, 1157–1179.

He, S., Pan, P., Dai, L., Wang, H., & Liu, J. (2012). Application of kernel-based Fisher discriminant analysis to map landslide susceptibility in the Qinggan River delta, Three Gorges, China. *Geomorphology, 171–172*, 30–41.

Kamp, U., Owen, L. A., Growley, B. J., & Khattak, G. A. (2010). Back analysis of landslide susceptibility zonation mapping for the 2005 Kashmir earthquake: an assessment of the reliability of susceptibility zoning maps. *Natural Hazards, 54*, 1–25.

Kanungo, D. P., Sarkar, S., & Sharma, S. (2011). Combining neural network with fuzzy, certainty factor and likelihood ratio concepts for spatial prediction of landslides. *Natural Hazards, 59*, 1491–1512.

Karimi, A. R., Mehrdadi, N., Hashemian, S. J., Bidhendi, G. N., & Moghaddam, R. T. (2011). Selection of wastewater treatment process based on the analytical hierarchy process and fuzzy analytical hierarchy process methods. *International Journal of Environmental Science & Technology, 8*, 267–280.

Kavzoglu, T., Sahin, E. K., & Colkesen, I. (2014). Landslide susceptibility mapping using GIS-based multi-criteria decision analysis, support vector machines, and logistic regression. *Landslides, 11*, 425–439.

Kayastha, P., Dhital, M. R., & De Smedt, F. (2012). Landslide susceptibility mapping using the weight of evidence method in the Tinau watershed, Nepal. *Natural Hazards, 63*, 479–498.

Kayastha, P., Dhital, M. R., & De Smedt, F. (2013). Application of the analytical hierarchy process (AHP) for landslide susceptibility mapping: A case study from the Tinau watershed, west Nepal. *Computers & Geosciences, 52*, 398–408.

Komac, M. (2006). A landslide susceptibility model using the Analytical Hierarchy Process method and multivariate statistics in perialpine Slovenia. *Geomorphology, 74*, 17–28.

Lee, S., & Pradhan, B. (2007). Landslide hazard mapping at Selangor, Malaysia using frequency ratio and logistic regression models. *Landslides, 4*, 33–41.

Lee, S., & Sambath, T. (2006). Landslide susceptibility mapping in the Damrei Romel area, Cambodia using frequency ratio and logistic regression models. *Environmental Geology, 50*, 847–855.

Lin, Z. C., & Shieh, T. J. (1995). Application of an analytical hierarchy process method and fuzzy compositional evaluation in the expert system of sheet bending design. *The International Journal of Advanced Manufacturing Technology, 10*, 3–10.

Ma, F., Wang, J., Yuan, R., Zhao, H., & Guo, J. (2013). Application of analytical hierarchy process and least-squares method for landslide susceptibility assessment along the Zhong-Wu natural gas pipeline, China. *Landslides, 10*, 481–492.

Meng, Q., Miao, F., Zhen, J., Wang, X., Wang, A., Peng, Y., & Fan, Q. (2015). GIS-based landslide susceptibility mapping with logistic regression, analytical hierarchy process, and combined fuzzy and support vector machine methods: A case study from Wolong Giant Panda Natural Reserve, China. *Bulletin of Engineering Geology and the Environment, 75*, 923–944. doi: 10.1007/s10064-015-0786-x

Mondal, S., & Maiti, R. (2013). Integrating the Analytical Hierarchy Process (AHP) and the frequency ratio (FR) model in landslide susceptibility mapping of Shiv-khola watershed, Darjeeling Himalaya. *International Journal of Disaster Risk Science, 4*, 200–212.

Nandi, A., & Shakoor, A. (2010). A GIS-based landslide susceptibility evaluation using bivariate and multivariate statistical analyses. *Engineering Geology, 110*, 11–20.

Nefeslioglu, H. A., Gokceoglu, C., & Sonmez, H. (2008). An assessment on the use of logistic regression and artificial neural networks with different sampling strategies for the preparation of landslide susceptibility maps. *Engineering Geology, 97*, 171–191.

Neuhäuser, B., & Terhorst, B. (2007). Landslide susceptibility assessment using "weights-of-evidence" applied to a study area at the Jurassic escarpment (SW-Germany). *Geomorphology, 86*, 12–24.

Nourani, V., Pradhan, B., Ghaffari, H., & Sharifi, S. S. (2014). Landslide susceptibility mapping at Zonouz Plain, Iran using genetic programming and comparison with frequency ratio, logistic regression, and artificial neural network models. *Natural Hazards, 71*, 523–547.

Ozdemir, A., & Altural, T. (2013). A comparative study of frequency ratio, weights of evidence and logistic regression methods for landslide susceptibility mapping: Sultan Mountains, SW Turkey. *Journal of Asian Earth Sciences, 64*, 180–197.

Park, S., Choi, C., Kim, B., & Kim, J. (2013). Landslide susceptibility mapping using frequency ratio, analytic hierarchy process, logistic regression, and artificial neural network methods at the Inje area, Korea. *Environmental Earth Sciences, 68*, 1443–1464.

Pourghasemi, H. R., Jirandeh, A. G., Pradhan, B., Xu, C., & Gokceoglu, C. (2013). Landslide susceptibility mapping using support vector machine and GIS at the Golestan Province, Iran. *Journal of Earth System Science, 122*, 349–369.

Pourghasemi, H. R., Moradi, H. R., Fatemi Aghda, S. F., Gokceoglu, C., & Pradhan, B. (2014). GIS-based landslide susceptibility mapping with probabilistic likelihood ratio and spatial multi-criteria evaluation models (North of Tehran, Iran). *Arabian Journal of Geosciences, 7*, 1857–1878.

Pourghasemi, H. R., Pradhan, B., & Gokceoglu, C. (2012). Application of fuzzy logic and analytical hierarchy process (AHP) to landslide susceptibility mapping at Haraz watershed, Iran. *Natural Hazards, 63*, 965–996.

Pradhan, B. (2013). A comparative study on the predictive ability of the decision tree, support vector machine and neuro-fuzzy models in landslide susceptibility mapping using GIS. *Computers & Geosciences, 51*, 350–365.

Pradhan, A. M. S., & Kim, Y. T. (2014). Relative effect method of landslide susceptibility zonation in weathered granite soil: A case study in Deokjeok-ri Creek, South Korea. *Natural Hazards, 72*, 1189–1217.

Pradhan, B., & Lee, S. (2010). Landslide susceptibility assessment and factor effect analysis: Backpropagation artificial neural networks and their comparison with frequency ratio and bivariate logistic regression modelling. *Environmental Modelling & Software, 25*, 747–759.

Pradhan, B., Oh, H. J., & Buchroithner, M. (2010). Weights-of-evidence model applied to landslide susceptibility mapping in a tropical hilly area. *Geomatics, Natural Hazards and Risk, 1*, 199–223.

Qiao, W., Li, W., & Zhang, X. (2014). Characteristic of water chemistry and hydrodynamics of deep karst and its influence on deep coal mining. *Arabian Journal of Geosciences, 7*, 1261–1275.

Rahimdel, M. J., & Ataei, M. (2014). Application of analytical hierarchy process to selection of primary crusher. *International Journal of Mining Science and Technology, 24*, 519–523.

Rahmati, O., Samani, A. N., Mahdavi, M., Pourghasemi, H. R., & Zeinivand, H. (2015). Groundwater potential mapping at Kurdistan region of Iran using analytic hierarchy process and GIS. *Arabian Journal of Geosciences, 8*, 7059–7071.

Robinson, T. P., van Klinken, R. D., & Metternicht, G. (2010). Comparison of alternative strategies for invasive species distribution modeling. *Ecological Modelling, 221*, 2261–2269.

Saadatkhah, N., Kassim, A., & Lee, L. M. (2015). Susceptibility assessment of shallow landslides in Hulu Kelang Area, Kuala Lumpur, Malaysia using analytical hierarchy process and frequency ratio. *Geotechnical and Geological Engineering, 33*, 43–57.

Saaty, T. L. (1980). *The analytic hierarchy process: Planning, priority setting, resources allocation*. New York, NY: McGraw-Hill.

Saito, H., Nakayama, D., & Matsuyama, H. (2009). Comparison of landslide susceptibility based on a decision-tree model and actual landslide occurrence: The Akaishi Mountains, Japan. *Geomorphology, 109*, 108–121.

Shahabi, H., Hashim, M., & Ahmad, B. B. (2015). Remote sensing and GIS-based landslide susceptibility mapping using frequency ratio, logistic regression, and fuzzy logic methods at the central Zab basin, Iran. *Environmental Earth Sciences, 73*, 8647–8668.

Solaimani, K., Mousavi, S. Z., & Kavian, A. (2013). Landslide susceptibility mapping based on frequency ratio and logistic regression models. *Arabian Journal of Geosciences, 6*, 2557–2569.

Süzen, M. L., & Doyuran, V. (2004). A comparison of the GIS based landslide susceptibility assessment methods: multivariate versus bivariate. *Environmental Geology, 45*, 665–679.

Tsangaratos, P., & Ilia, I. (2015). Landslide susceptibility mapping using a modified decision tree classifier in the Xanthi Perfection. *Greece. Landslides,* 1–16.

van Westen, C. J., Rengers, N., & Soeters, R. (2003). Use of geomorphological information in indirect landslide susceptibility assessment. *Natural Hazards, 30*, 399–419.

van Westen, C. J., van Asch, T. W., & Soeters, R. (2006). Landslide hazard and risk zonation – Why is it still so difficult? *Bulletin of Engineering Geology and the Environment, 65*, 167–184.

Wang, Q., Li, W., Chen, W., & Bai, H. (2015). GIS-based assessment of landslide susceptibility using certainty factor and index of entropy models for the Qianyang County of Baoji city, China. *Journal of Earth System Science, 124*, 1399–1415.

Xie, Y. (2013). *Characteristic analysis and risk assessment of geological disaster in Wen county*(Master's thesis). Lanzhou University, Lanzhou. 19 p.

Yalcin, A. (2008). GIS-based landslide susceptibility mapping using analytical hierarchy process and bivariate statistics in Ardesen (Turkey): Comparisons of results and confirmations. *CATENA, 72*, 1–12.

Yalcin, A., Reis, S., Aydinoglu, A. C., & Yomralioglu, T. (2011). A GIS-based comparative study of frequency ratio, analytical hierarchy process, bivariate statistics and logistics regression methods for landslide susceptibility mapping in Trabzon, NE Turkey. *CATENA, 85*, 274–287.

Yang, Z. H., Lan, H. X., Gao, X., Li, L. P., Meng, Y. S., & Wu, Y. M. (2015). Urgent landslide susceptibility assessment in the 2013 Lushan earthquake-impacted area, Sichuan Province, China. *Natural Hazards, 75*, 2467–2487.

Yao, X., Tham, L. G., & Dai, F. C. (2008). Landslide susceptibility mapping based on Support Vector Machine: A case study on natural slopes of Hong Kong, China. *Geomorphology, 101*, 572–582.

Yilmaz, I. (2009). Landslide susceptibility mapping using frequency ratio, logistic regression, artificial neural networks and their comparison: A case study from Kat landslides (Tokat—Turkey). *Computers & Geosciences, 35*, 1125–1138.

Yilmaz, C., Topal, T., & Süzen, M. L. (2012). GIS-based landslide susceptibility mapping using bivariate statistical analysis in Devrek (Zonguldak-Turkey). *Environmental Earth Sciences, 65*, 2161–2178.

Youssef, A. M. (2015). Landslide susceptibility delineation in the Ar-Rayth area, Jizan, Kingdom of Saudi Arabia, using analytical hierarchy process, frequency ratio, and logistic regression models. *Environmental Earth Sciences, 73*, 8499–8518.

Youssef, A. M., Al-Kathery, M., & Pradhan, B. (2015). Landslide susceptibility mapping at Al-Hasher area, Jizan (Saudi Arabia) using GIS-based frequency ratio and index of entropy models. *Geosciences Journal, 19*, 113–134.

Youssef, A. M., Pourghasemi, H. R., El-Haddad, B. A., & Dhahry, B. K. (2015). Landslide susceptibility maps using different probabilistic and bivariate statistical models and comparison of their performance at Wadi Itwad Basin, Asir Region, Saudi Arabia. *Bulletin of Engineering Geology and the Environment,* 1–25.

Zhang, Y., Sun, Y., & Qin, J. (2012). Sustainable development of coal cities in Heilongjiang province based on AHP method. *International Journal of Mining Science and Technology, 22*, 133–137.